Spin Relaxation Studies with the HERMES Internal Polarized Deuterium Target

C. Baumgarten[1] on behalf of the HERMES collaboration

October 1, 1999

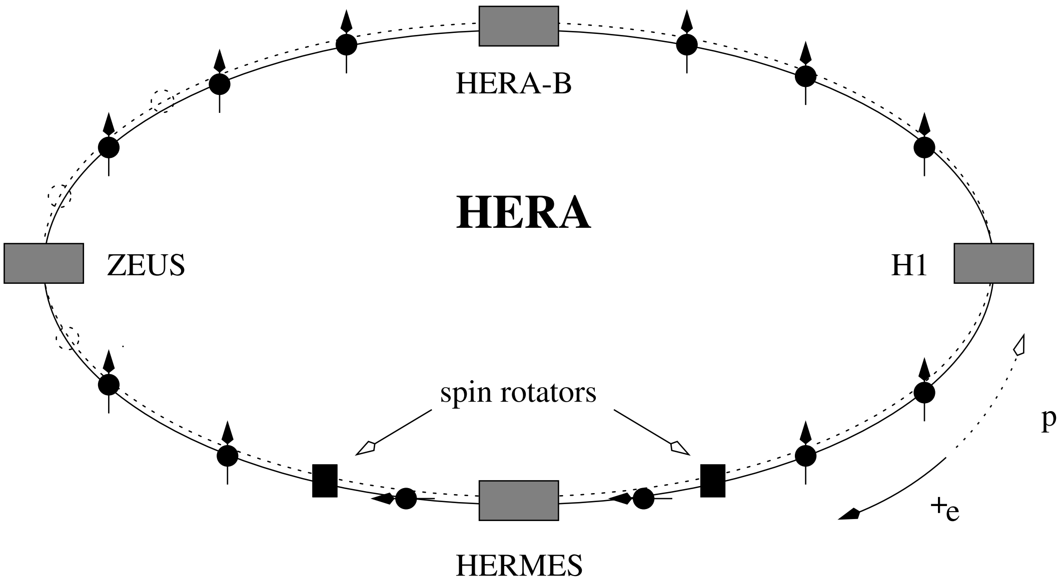

- Overview of hardware setup
- Calibration of the target polarimeter (BRP)
- Data modelling
- Results
- Summary

1) Ludwig-Maximilians Universität München.

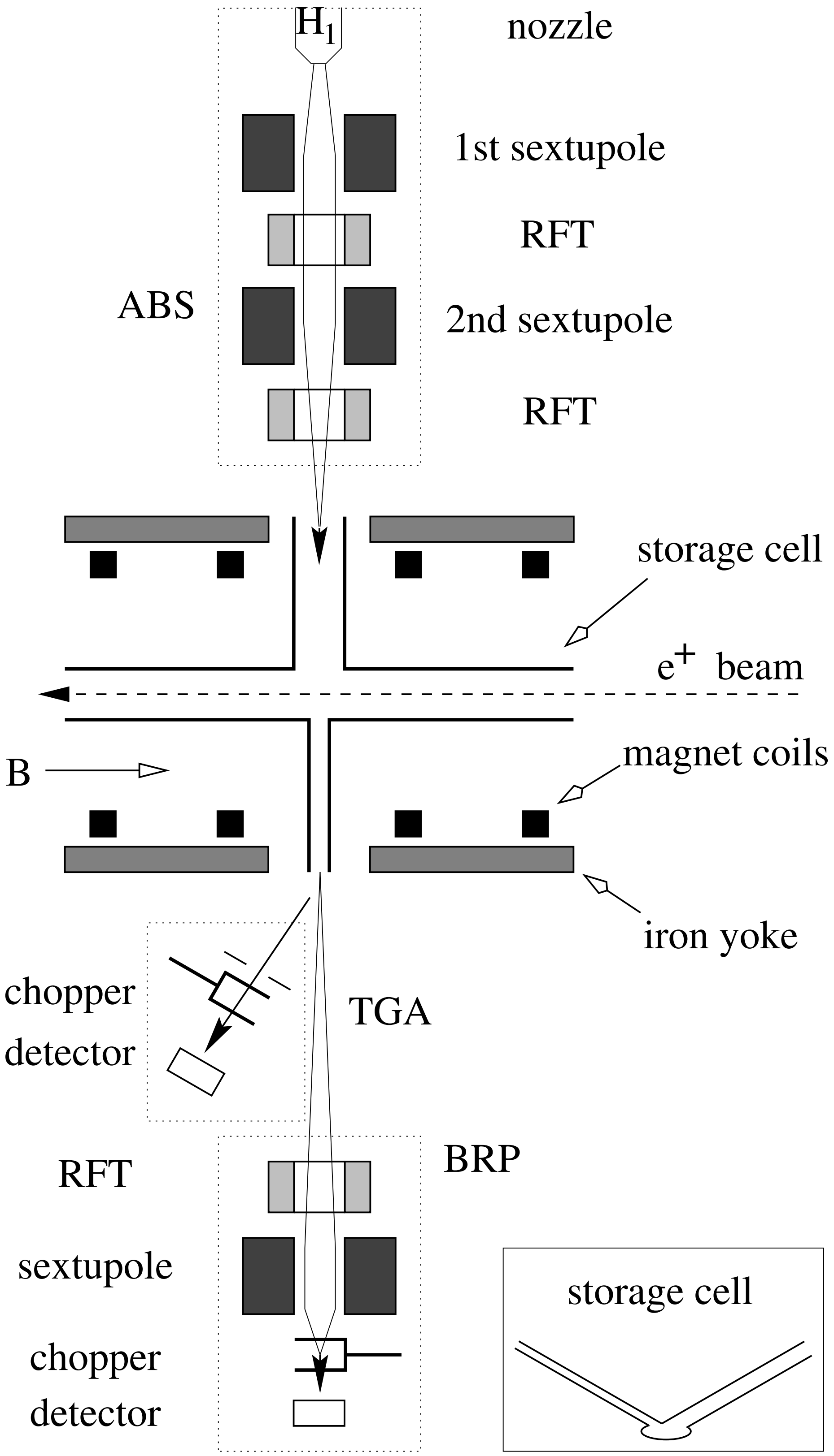
H_1
nozzle
1st sextupole
RFT
ABS
2nd sextupole
RFT
storage cell
e^+ beam
magnet coils
B
iron yoke
chopper
detector
TGA
BRP
RFT
sextupole
chopper
detector
storage cell

The Storage Cell and Target Holding Field Magnet

- Cell walls made out of 75 μm thick aluminum (hadrons detectable).
- Drifilm coating to minimize wall depolarization and recombination.
- Helium cooled cell - temperature range of $34 \ldots 300\,K$.
- Holding field range $0 \ldots 350\,mT$.

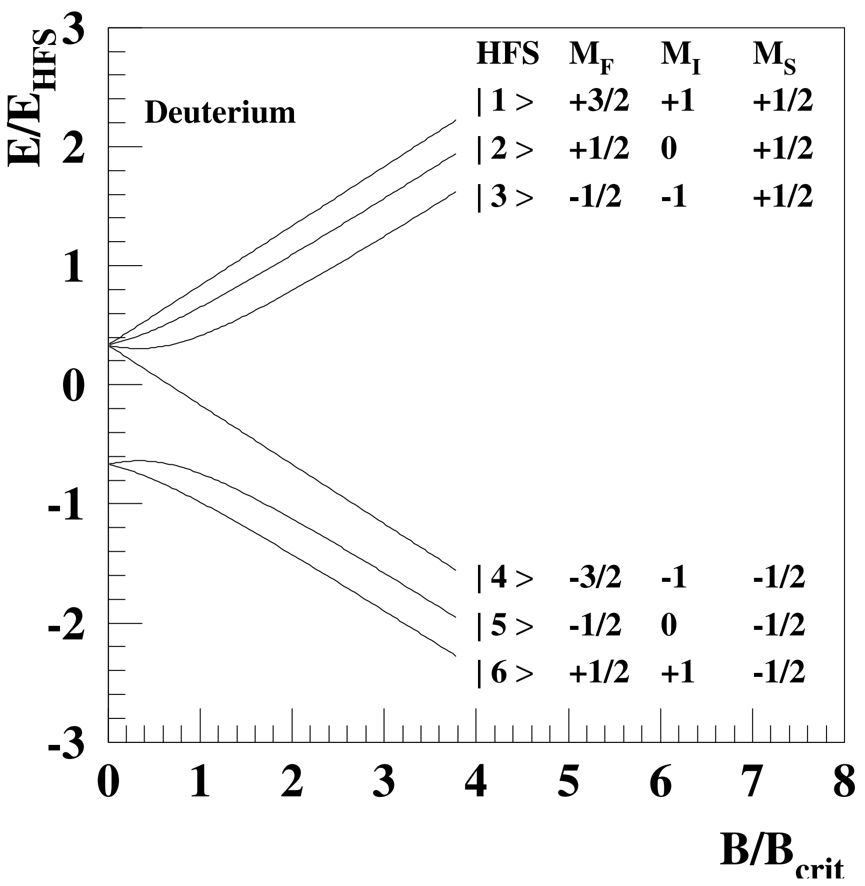

The Atomic Beam Source (ABS)

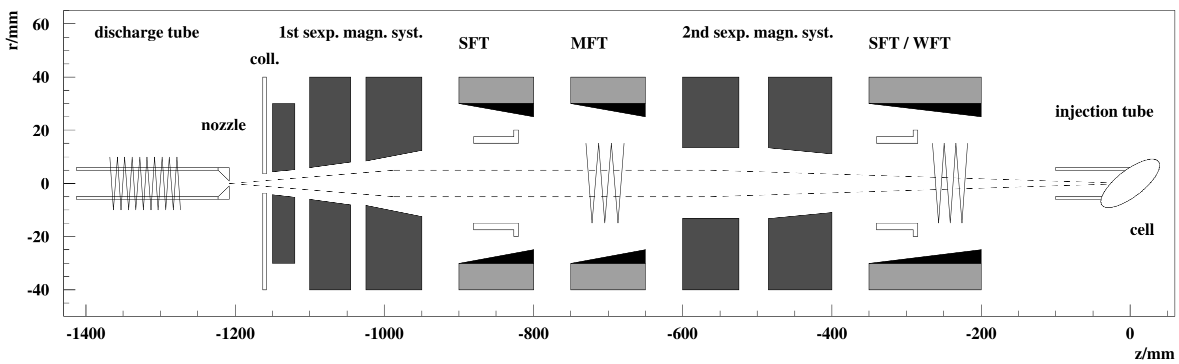

- RF dissociator with $\simeq 80\%$ degree of dissociation.
- 5 (tapered) magnets in 2 subsystems.
- 4 transition units, 3 of them independently operational.
- $\vec{D}$ beam intensity $\sim 3.5 \cdot 10^{16}\, nuc\, s^{-1}$ (3 hyperfine states).

Default Injection Modes:

Pol.	Inj. HFS	high frequency transitions	
		appendix	between sextupole subsystems
P_e	$\|1\rangle, \|2\rangle, \|3\rangle$	OFF	OFF
P_{z+}	$\|1\rangle, \|6\rangle$	SFT 2-6 (**s26**)	SFT 3-5 (**t35**)
P_{z-}	$\|3\rangle, \|4\rangle$	WFT 1-4/2-3 (**w14**)	SFT 3-5 (**t35**)
P_{zz+}	$\|3\rangle, \|6\rangle$	SFT 2-6 (**s26**)	MFT 1-4 (**m14**)
P_{zz-}	$\|2\rangle, \|5\rangle$	SFT 3-5 (**s35**)	MFT 1-4 (**m14**)
P_{e+}, P_{z+}	$\|1\rangle$	OFF	MFT 3-4 (**m34**), SFT 2-6 (**t26**)
P_{e+}, P_{zz-}	$\|2\rangle$	OFF	WFT 1-4/2-3 (**v14**), SFT 2-6 (**t26**)
P_{e+}, P_{z-}	$\|3\rangle$	OFF	WFT 1-4/2-3 (**v14**), SFT 3-5 (**t35**)
P_{e-}, P_{z-}	$\|4\rangle$	WFT 1-4/2-3 (**w14**)	MFT 3-4 (**m34**), SFT 2-6 (**t26**)
P_{e-}, P_{zz-}	$\|5\rangle$	SFT 3-5 (**s35**)	WFT 1-4/2-3 (**v14**), SFT 2-6 (**t26**)
P_{e-}, P_{z+}	$\|6\rangle$	SFT 2-6 (**s26**)	WFT 1-4/2-3 (**v14**), SFT 3-5 (**t35**)

The Breit-Rabi Type Polarimeter (BRP)

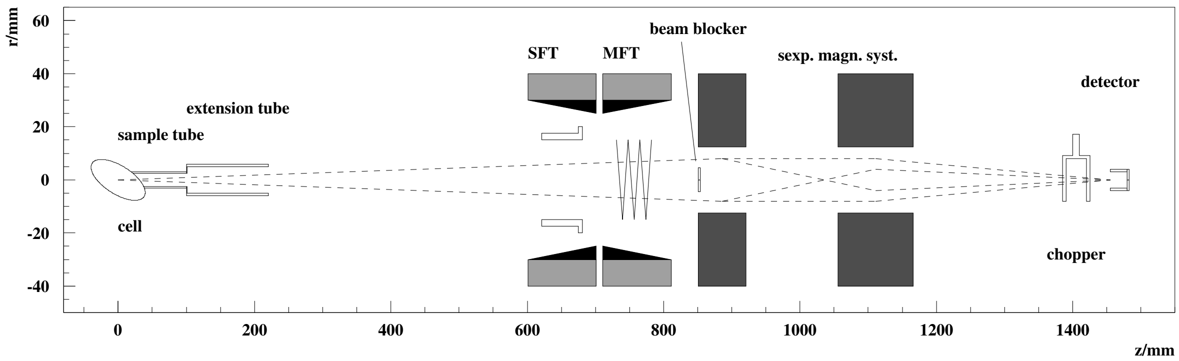

Task

Measure polarization of sample beam.

Measurement

- Use chopper to substract background.
- Measure RFT off - signal = $N_1 + N_2 + N_3$.
- Measure SFT 1-6 on - signal = $N_2 + N_3 + N_6$ (etc).
- $\rightarrow$ Linear equation system, solution $\rightarrow N_i$.

Calibration

- $N_{sig} > N_{HFS}$ $\rightarrow$ system overdetermined.
- $\rightarrow$ add. parameters - efficiencies - can be fitted.

Performance

- Min. time for a measurement $\sim 45\, s$.
- Stat. error in 2 min $\sim 2\%$.

Syst. uncert. of measured vector polarization $\simeq 1\%$.

Results of BRP Calibration

Due to Cross-Talk of Static Magnetic Field of Transition units the MFTs need to be tuned and calibrated for each SFT operation mode seperately.

- MFT 1-4, MFT 2-4, MFT 3-4 $\rightarrow$ 9 Efficiencies / SFT
- 4 SFTs: SFT 1-6, SFT 2-6, SFT 2-5/3-6, SFT 3-5
- Number of Efficiencies = 5 SFTs + 4 x 9 MFTs = 41.
- All Efficiencies $\geq 90\,\%$ (except $\varepsilon_{s36} = 0.804$).
- Typical uncertainty $1 \ldots 2\,\%$.
- For example: $\varepsilon_{s16} = 0.986 \pm 0.012$.
- Results are highly correlated $\rightarrow$ correlations reduce total uncertainty.

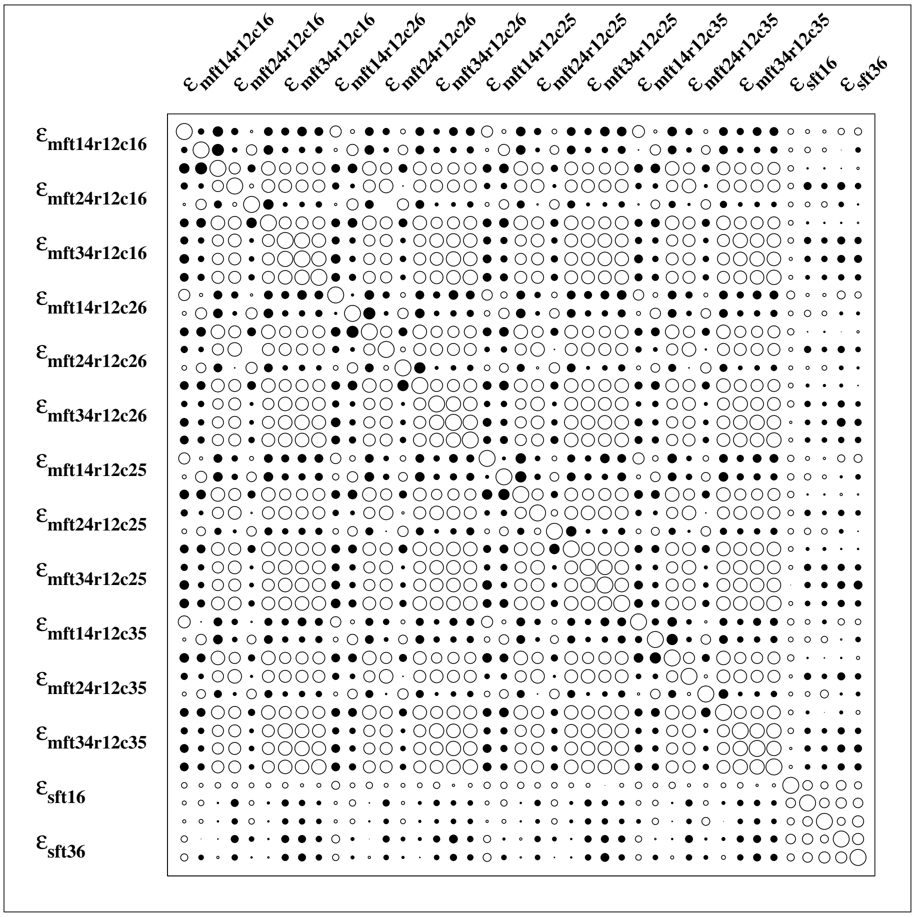

TOF measurements using pulsed hyperfine transitions

Signal with MFT transition in BRP off:

$$\begin{pmatrix}0\\0\\1\\1\\0\\0\end{pmatrix} \overset{\text{BRP SFT 3-5}}{\rightarrow} \begin{pmatrix}0\\0\\0\\1\\1\\0\end{pmatrix} \overset{\text{BRP sextupoles}}{\rightarrow} \begin{pmatrix}0\\0\\0\\0\\0\\0\end{pmatrix} .$$

Signal with MFT transition in BRP on:

$$\begin{pmatrix}0\\0\\1\\1\\0\\0\end{pmatrix} \overset{\text{BRP SFT 3-5}}{\rightarrow} \begin{pmatrix}0\\0\\0\\1\\1\\0\end{pmatrix} \overset{\text{BRP MFT 3-4}}{\rightarrow} \begin{pmatrix}0\\0\\1\\0\\1\\0\end{pmatrix} \overset{\text{BRP sextupoles}}{\rightarrow} \begin{pmatrix}0\\0\\1\\0\\0\\0\end{pmatrix} .$$

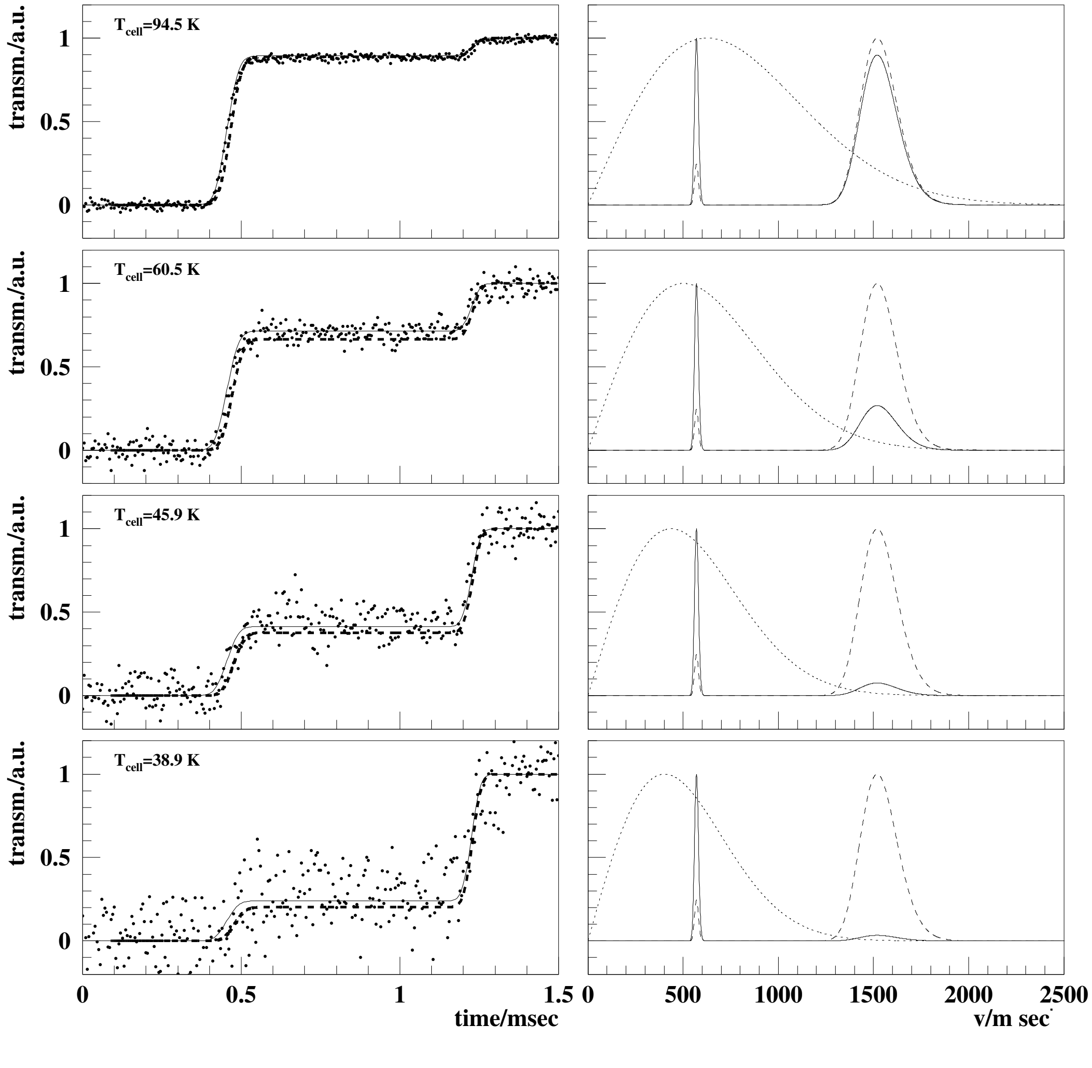

Measurement of Diffusion Time τ_d in Target Cell

WFT between sextupole subsystems of ABS off:

$$\begin{pmatrix}1\\1\\1\\1\\1\\1\end{pmatrix} \overset{\text{1st sixp.}}{\rightarrow} \begin{pmatrix}1\\1\\1\\0\\0\\0\end{pmatrix} \overset{\text{ABS SFT 3-5}}{\rightarrow} \begin{pmatrix}1\\1\\0\\0\\1\\0\end{pmatrix} \overset{\text{2nd sixp.}}{\rightarrow} \begin{pmatrix}1\\1\\0\\0\\0\\0\end{pmatrix}.$$

WFT between sextupole subsystems of ABS on:

$$\begin{pmatrix}1\\1\\1\\1\\1\\1\end{pmatrix} \overset{\text{1st sixp.}}{\rightarrow} \begin{pmatrix}1\\1\\1\\0\\0\\0\end{pmatrix} \overset{\text{ABS SFT 3-5}}{\rightarrow} \begin{pmatrix}1\\1\\0\\0\\1\\0\end{pmatrix} \overset{\text{ABS WFT 1-4/2-3}}{\rightarrow} \begin{pmatrix}0\\0\\1\\1\\1\\0\end{pmatrix} \overset{\text{2nd sixp.}}{\rightarrow} \begin{pmatrix}0\\0\\1\\0\\0\\0\end{pmatrix}.$$

Monte Carlo: Diffusion length $L_d = \langle\, v \,\rangle\, \tau_d \simeq 410\, cm.$

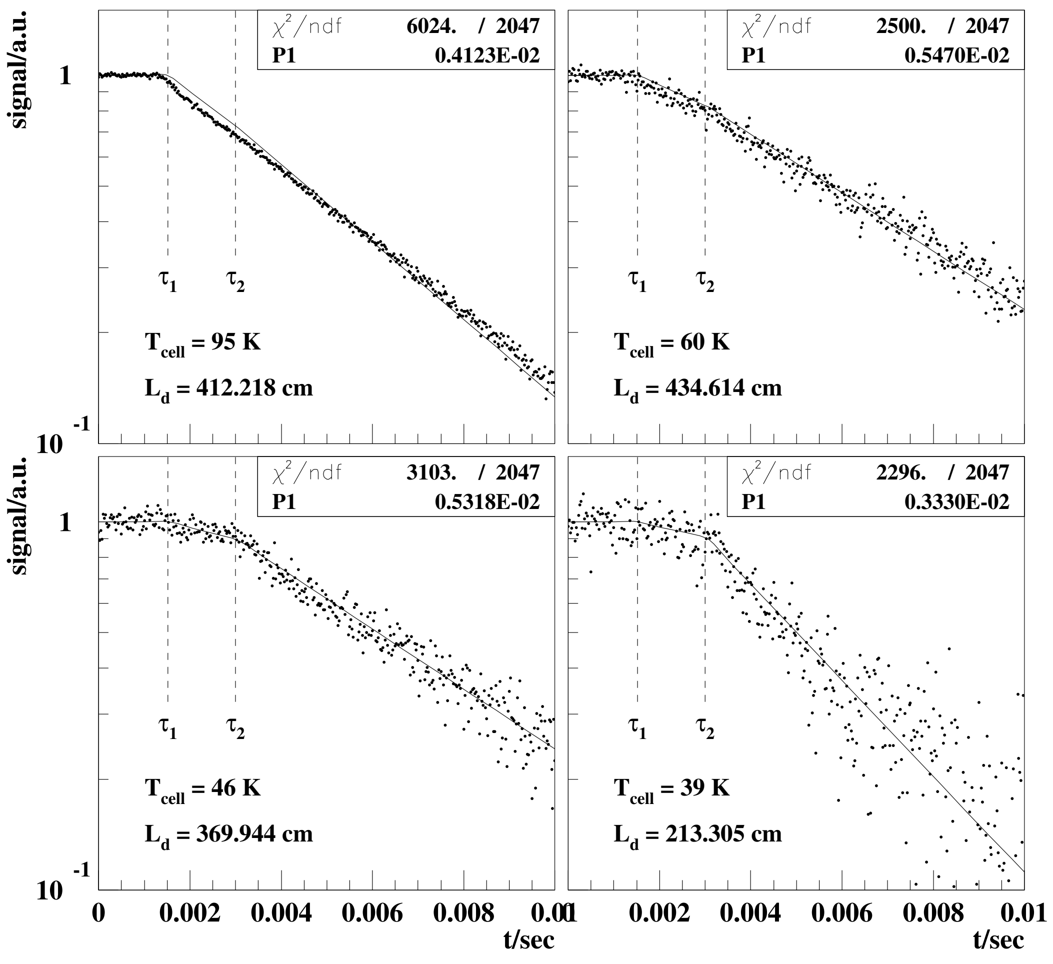

Spin relaxation model

Task

- Model/understand relaxation processes inside HERMES storage cell.
- Compare to measured data like magnetic field scan.
- Investigate effect of spin exchange and wall depolarization.
- Fit injected polarization.

Relaxation time model

$$0 = \frac{N_a^{inj} - N_a}{\tau_d} + \frac{1}{\tau_f} \sum_b R_{ab} N_b + \frac{1}{\tau_{se}} \sum_{b,c} M_{bc}^a N_b N_c \,.$$

- N_a: Hyperfine Occupation of state $|\, a \,\rangle$.
- τ_d: Diffusion time.
- τ_f: Time of flight between wall collisions.
- τ_{se}: Spin exchange relaxation time.
- $\sum_b R_{ab}\, N_b = \sum_b W_{b \to a} N_b - N_a \sum_b W_{b \to a}$: Wall depolarization term.
- $\sum_{b,c} M_{bc}^a\, N_b\, N_c$: Spin exchange term (Purcell/Fields, Walker/Anderson).

Wall Relaxation

Concepts:

1. Bouchiat / Brossel: Variation of the local magnetic field induces hyperfine transitions:

$$\mathcal{H} \propto \gamma_S \vec{S} \vec{B}_{loc} \,.$$

2. Bloembergen/Purcell/Pound (a): Interaction with dipols of nucleons on the surface (similar to spin-spin-relaxation):

$$\mathcal{H} \propto \gamma_S \gamma_I \frac{\vec{S}\vec{I} - (\vec{n}\vec{S})(\vec{n}\vec{I})}{r^3} \,.$$

(Total angular momentum is conserved: $\Delta m_S + \Delta m_I = 0$.)

3. Bloembergen/Purcell/Pound (b): Time dependent dipol-dipol interaction is equivalent to interaction with lattice vibrations of the solid (similar to spin-lattice-relaxation):

$$\mathcal{H} \propto \gamma_S \gamma_I \frac{\vec{S}\vec{I} - (\vec{n}\vec{S})(\vec{n}\vec{I})}{r^3(t)} \,.$$

(Total angular momentum is not conserved.)

All concepts lead to:

$$W_{b \to a} = C_{wall} \, \tau_S \, j(\omega_{ab}) \, | \, \langle \, a \, | \, \vec{S}_{op} \, | \, b \, \rangle \, |^2 \,.$$

Spectral Densities

C.A. Scholl:

- 2-dimensional diffusion, low frequency limit:

$$J^{(p)}(\omega) \propto \tau_c \log\left(1 + \frac{1}{\omega^2\tau_c^2}\right).$$

- 3-dimensional diffusion, low frequency limit:

$$J^{(p)}(\omega) \propto \frac{2\tau_c}{1+\omega^2\tau_c^2} \to 2\tau_c\,.$$

- Spin-lattice relaxation (2-dim. diffusion):

$$j(\omega) \propto [J^{(1)}(\omega) + J^{(2)}(2\omega)] \propto \log\left(1 + \frac{1}{\omega^2\tau_c^2}\right).$$

- Spin-spin relaxation (2-dim. diffusion):

$$j(\omega) \propto [J^{(0)}(0) + 10\, J^{(1)}(\omega) + J^{(2)}(2\omega)] = \tau_c \left(A + B \log\left(1 + \frac{1}{\omega^2\tau_c^2}\right)\right).$$

- Spin-lattice relaxation (2-dim./3-dim. diffusion):

$$j(\omega) \propto \tau_c \left(A + B \log\left(1 + \frac{1}{\omega^2\tau_c^2}\right)\right).$$

Measurement of Spectral Density

- Assuming, the injected hyperfine occupation is known.
- $\omega_{ab} = \omega_{ab}(B) \;\rightarrow$ measure relax. vs. field.
- Fit $j(\omega_{ab}(B_i))$ for all possible 10 hyperfine transitions.

$$j(\omega) \propto \log\left(1 + \frac{1}{\omega^2 \tau_c^2}\right)$$

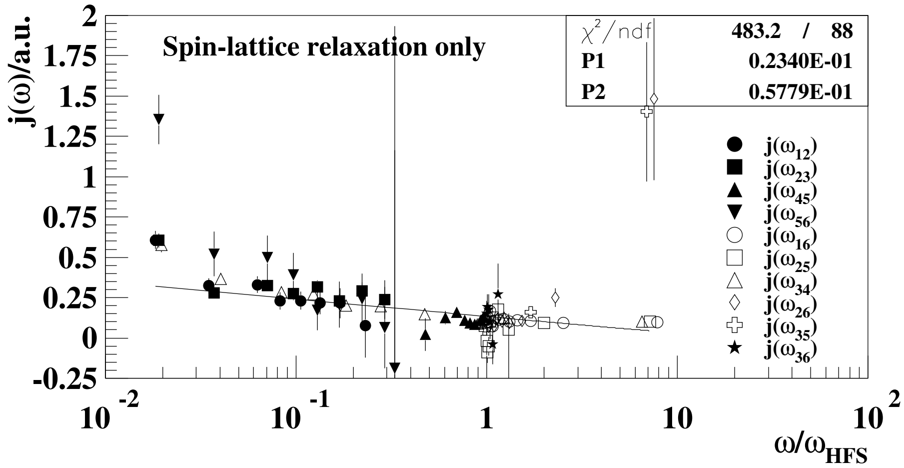

$$j(\omega) = A + B\log\left(1 + \frac{1}{\omega^2 \tau_c^2}\right)$$

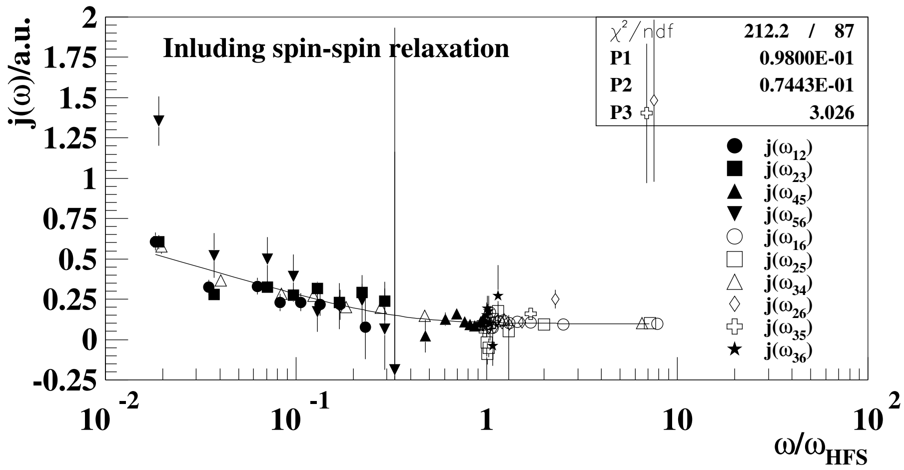

Measurement of sticking time

Sticking time τ_s given by Arrhenius law:

$$\tau_s = \tau_s^0 \, \exp\left(\frac{E_b}{k_b T}\right)$$

with binding energy E_b:

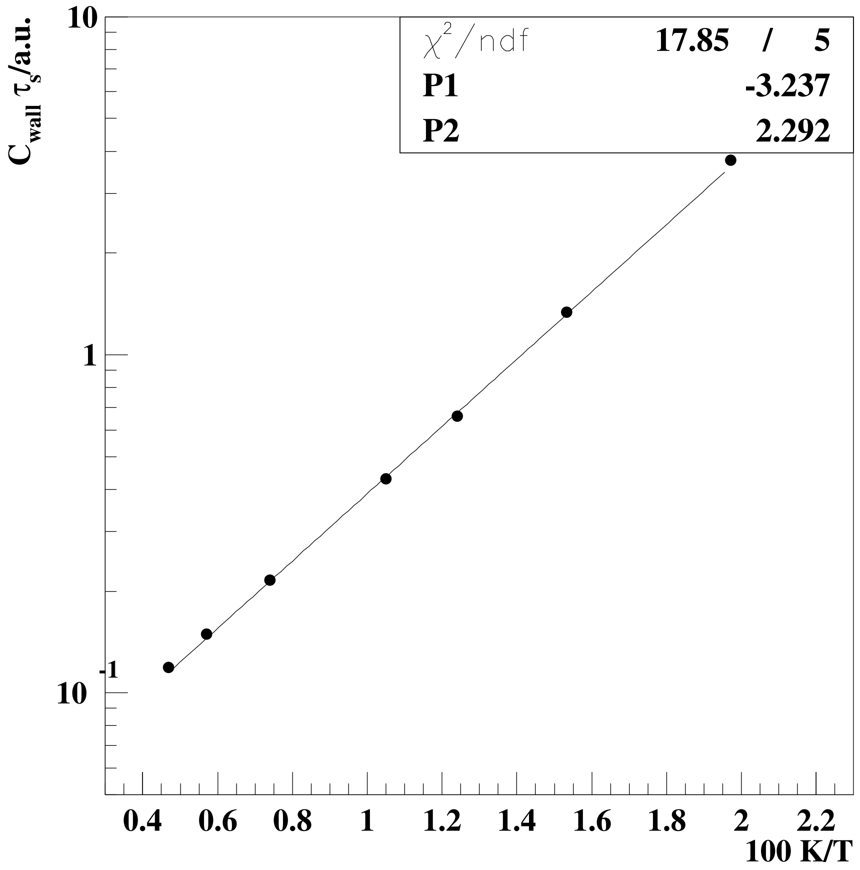

Resulting binding energy $E_b = 19.7\,meV$.

<u>**Relaxation Modell ↔ Data**</u>

Measure hyperfine occupation at

- of 11 different injection modes of ABS
- at 10 different values of magnetic holding field
- at 8 different values of storage cell temperatures

At a cell temperature of $95\,K$:

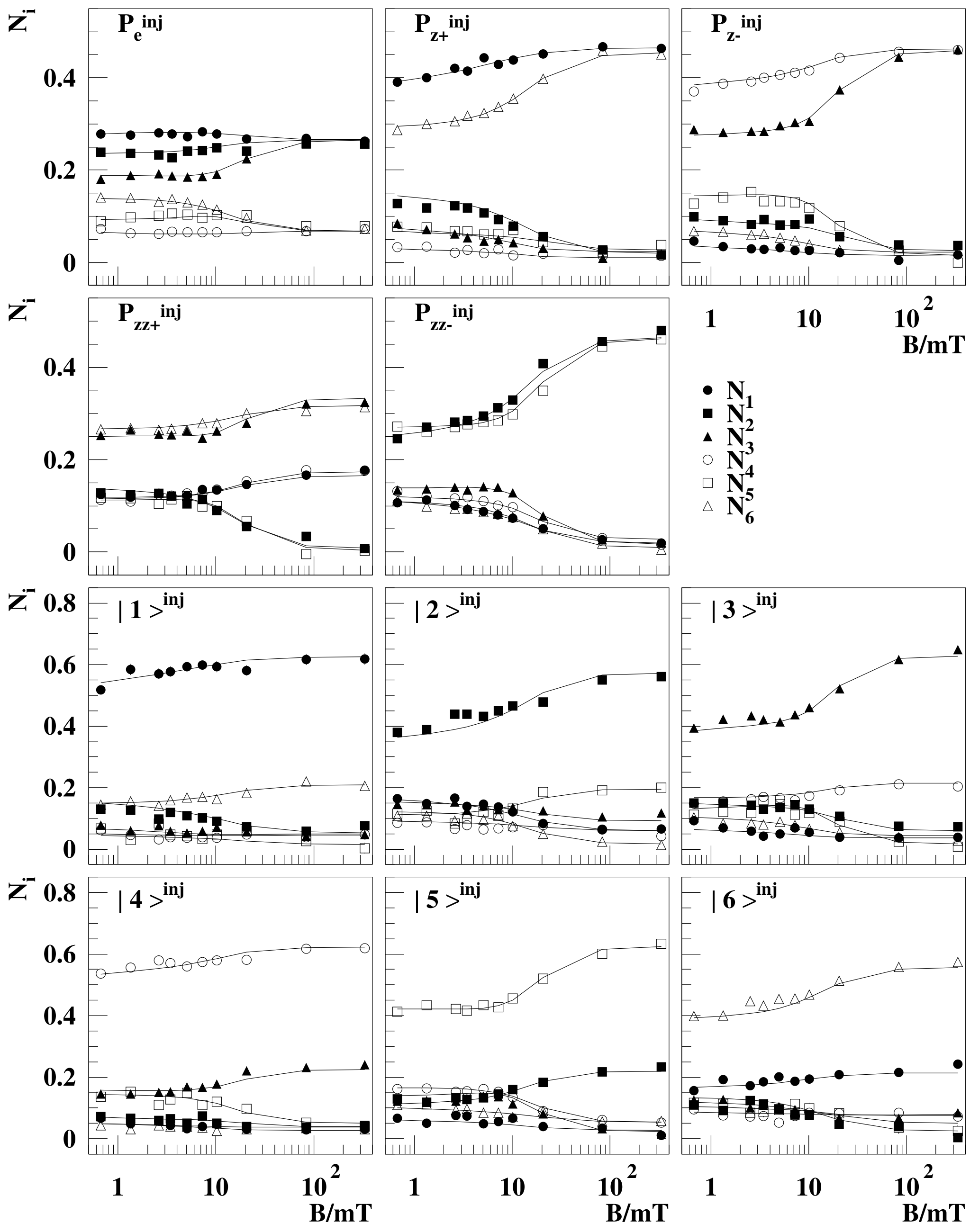

Temperature Dependance of Polarization

At a holding field of $335\,mT$:

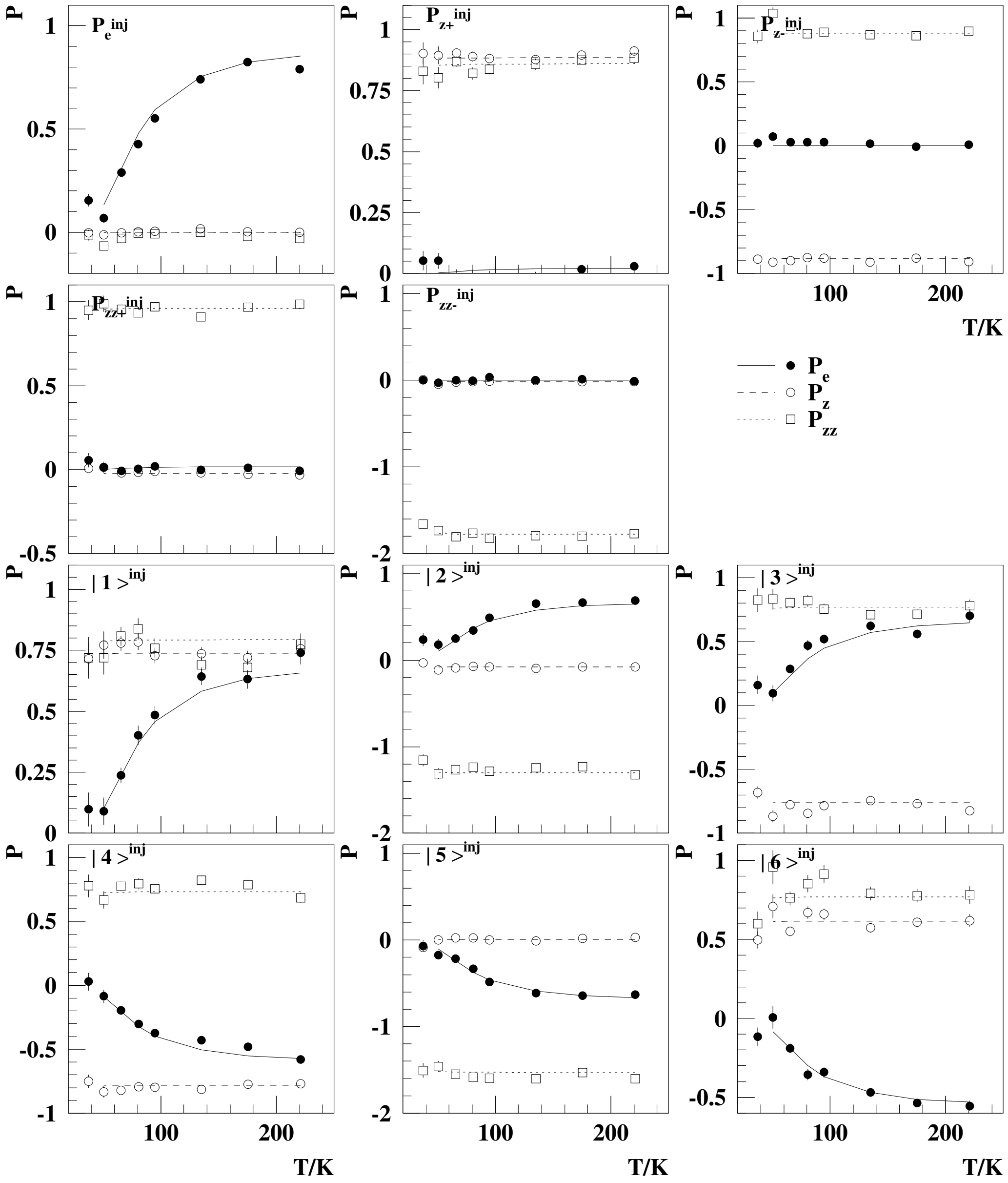

Problem:

At low temperatures ($\leq 40\,K$) the model does not (yet) match data.

Fitted Parameters

- ABS transition efficiencies.
- Wall depolarization strength (resp. average sticking time τ_s)
- Coefficients of spectral density of wall depolarization
- Spin exchange rel. time, resp. atomic target density

Results:

- ABS transition efficiencies are high, for example $\varepsilon_{s35} = 98.2 \pm 0.34\,\%$.
- Injected vector polarization:

$$P_{z+}^{inj} = 88.49 \pm 0.20\,\%$$

$$P_{z-}^{inj} = -88.32 \pm 0.72\,\%$$

- No measurable depolarization of $P_{z\pm}$ at high holding field.
- $\rightarrow$ Sampling correction C_P of pol. at working point $C_P = 1$.

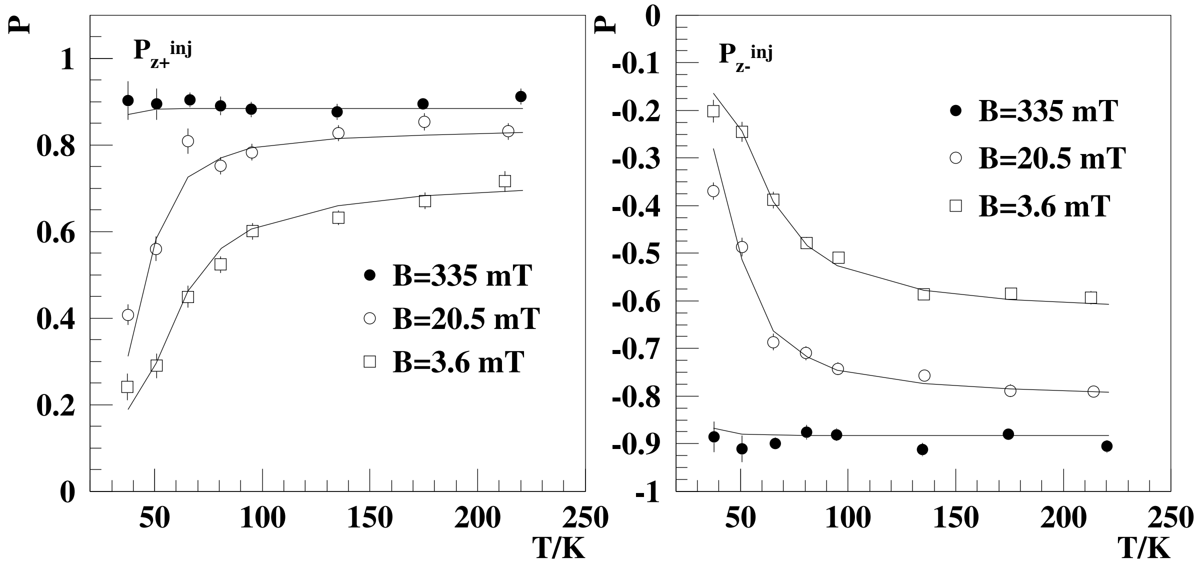

Summary

- Breit-Rabi Polarimeter (BRP) could be calibrated for $\vec{D}$ operation.
- The resulting syst. uncertainty of measured vector pol. is $\simeq \pm 1\,\%$ (absolute).
- The sextupole system of BRP can be analysed by TOF measurements. The data are consistent with a Maxwellian velocity distribution.
- The diffusion time of the atoms entering the BRP could be measured. The result is consistent with the prediction of the molecular flow simulation.
- The spin relaxation processes as function of holding field and storage cell temperature could be modelled and are reasonably well understood, except for very low temperatures.
- The spectral density of the wall relaxation could be measured and is in reasonable agreement with the assumption of 2-dim. diffusion.
- The transition efficiencies of the ABS could be determined.
- Injected nuclear polarization is high $P_{z\pm}^{inj} \simeq \pm 88.5\%$.
- No measurable polarization loss at target working point.
- Syst. uncertainty of the atomic target polarization equals the syst. uncert. of BRP measurement.

ABS transition efficiencies (1998)

ε_{s26}	$97.4 \pm 0.41\,\%$
ε_{s35}	$98.2 \pm 0.34\,\%$
ε_{t26}	$93.0 \pm 0.73\,\%$
ε_{t35}	$94.5 \pm 0.5\,\%$
ε_{v14r12}	100%
ε_{v14r23}	100%
ε_{v14r34}	100%
ε_{v14r13}	$96.95 \pm 0.53\,\%$
ε_{v14r24}	100.0%
ε_{v14r14}	$91.8 \pm 0.39\,\%$
ε_{w14r12}	100%
ε_{w14r23}	100%
ε_{w14r34}	100%
ε_{w14r13}	$97.7 \pm 1.0\,\%$
ε_{w14r24}	100.0%
ε_{w14r14}	$77.6 \pm 7.4\,\%$
ε_{w14r56}	$82.5 \pm 7.6\,\%$
ε_{m14r12}	$98.4 \pm 0.42\,\%$
ε_{m14r23}	$99.2 \pm 0.39\,\%$
ε_{m14r34}	$98.3 \pm 0.18\,\%$
ε_{m34r34}	$97.1 \pm 0.46\,\%$

Injected Polarization

Mode	P_e	P_z	P_{zz}	Rel. Int.
P_e	100.00 ± 0.00	0.00 ± 0.00	0.00 ± 0.00	100.00 ± 0.00
P_{z+}	2.44 ± 0.46	88.49 ± 0.20	86.08 ± 0.73	71.57 ± 0.15
P_{z-}	0.01 ± 0.25	-88.32 ± 0.71	87.87 ± 1.64	71.57 ± 0.15
P_{zz+}	2.03 ± 0.54	-2.38 ± 0.41	96.35 ± 0.59	70.44 ± 0.05
P_{zz-}	0.44 ± 0.48	-1.58 ± 0.32	-178.24 ± 0.91	70.44 ± 0.05
$\vert 1 \rangle$	76.98 ± 1.18	73.83 ± 0.35	79.35 ± 0.95	42.82 ± 0.26
$\vert 2 \rangle$	76.14 ± 1.02	-7.63 ± 0.78	-130.40 ± 1.38	41.95 ± 0.22
$\vert 3 \rangle$	75.70 ± 0.70	-76.25 ± 0.51	77.05 ± 1.16	41.50 ± 0.15
$\vert 4 \rangle$	-66.95 ± 0.28	-78.25 ± 1.08	73.18 ± 1.68	42.82 ± 0.26
$\vert 5 \rangle$	-77.75 ± 0.95	0.47 ± 0.27	-153.12 ± 1.51	41.50 ± 0.15
$\vert 6 \rangle$	-62.24 ± 1.10	61.57 ± 0.84	77.18 ± 1.38	41.95 ± 0.22

Injected Hyperfine Occupation

Mode	N_1	N_2	N_3	N_4	N_5	N_6
P_e	33.3 ± 0.0	33.3 ± 0.0	33.3 ± 0.0	0.0 ± 0.0	0.0 ± 0.0	0.0 ± 0.0
P_{z+}	46.6 ± 0.1	1.2 ± 0.1	3.4 ± 0.2	0.0 ± 0.1	3.4 ± 0.1	45.4 ± 0.3
P_{z-}	1.0 ± 0.3	3.4 ± 0.4	45.6 ± 0.6	46.6 ± 0.2	0.6 ± 0.3	2.8 ± 0.3
P_{zz+}	2.8 ± 0.2	1.2 ± 0.2	47.0 ± 0.3	3.6 ± 0.1	0.0 ± 0.1	45.4 ± 0.4
P_{zz-}	2.8 ± 0.2	46.6 ± 0.3	0.8 ± 0.1	3.6 ± 0.1	46.2 ± 0.4	0.0 ± 0.1
$\vert 1 \rangle$	77.8 ± 0.0	6.9 ± 0.6	3.8 ± 0.4	5.9 ± 0.0	0.0 ± 0.0	5.6 ± 0.0
$\vert 2 \rangle$	7.8 ± 0.3	71.1 ± 0.8	9.2 ± 0.7	6.2 ± 0.3	5.7 ± 0.3	0.0 ± 0.3
$\vert 3 \rangle$	2.1 ± 0.3	7.6 ± 0.4	78.1 ± 0.7	6.2 ± 0.3	0.0 ± 0.3	5.9 ± 0.3
$\vert 4 \rangle$	5.4 ± 0.2	4.3 ± 0.3	6.8 ± 0.6	77.8 ± 0.0	4.6 ± 0.4	1.0 ± 0.4
$\vert 5 \rangle$	2.1 ± 0.3	7.6 ± 0.4	1.3 ± 0.3	6.2 ± 0.3	76.7 ± 0.8	5.9 ± 0.3
$\vert 6 \rangle$	7.8 ± 0.3	1.9 ± 0.3	9.2 ± 0.7	6.2 ± 0.3	5.7 ± 0.3	69.2 ± 0.9